

Graphene oxide for room temperature CO, H₂ and UV sensing

ABDELRAHIM ATE, ZHENAN TANG*

School of Electronic Science and Technology, Faculty of Electronic Information and Electrical Engineering, Dalian University of Technology, Dalian 116024, P.R. China

Improved Hummers technique employed for the synthesis of graphene oxide, the morphology, structure and composition characterized by (TEM) and (SEM). The device sensor fabricated by dispersing graphene oxide on an interdigitated Au-electrode for both gas and UV sensing. A graphene oxide gas sensor based on CO, H₂ and UV photodetector exhibited excellent responsivity, fast response and recovery time. The gas sensor sensitivities were around 17.12% and 22.83% for different gas (CO, H₂) concentrations at room temperature; as well the sensor resistance decreased in exposure to CO and H₂, revealing p-type semiconducting behaviour of the graphene oxide as excellent materials.

(Received September 9, 2015, accepted October 28, 2015)

Keywords: Graphene oxide, Gas sensor, UV photodetector

1. Introduction

Graphene Oxide (GO) is a single-atomic-layered material made by the oxidation of graphite crystals [1]. It was one of the first commercial graphene materials, due to the fact that it is both inexpensive and one of the most popular products on the graphene market. It will play an important role in the development of the next generation of graphene materials, thanks to its cost-effectiveness, carbon-base, flexibility, and transparent electronics. It is the strongest material available, with high transparency, and it is a superior thermal and electrical conductor [2-5]. Produce in bulk quantities it would be cost-effective and advantageous both for industry and commerce.

Graphene oxide is also characterized by low-cost, high spread ability to convert to graphene, easy access and the ability to disperse in deionized water [6, 7].

The atom-thick two-dimensional conjugated structures, high conductivity, and large specific surface areas of the graphene materials have been widely used for fabrication of gas sensors [8,9], transparent conductive films [10], paper-like and composite materials [11], energy-related materials [12], antibacterial materials [13], biological, photonics and optoelectronics and medical applications [14,15].

It is possible to deposit graphene oxide films on any substrate, and then convert it into a conductor. These coatings used in solar cells [16], electrode materials [17], flexible electronics and chemical sensors [18]. Graphene can be prepared by a number of methods, such as micromechanical exfoliation [19], epitaxial growth on silicon carbide [20], chemical vapour deposition (CVD) [21], arc discharge method

[22], plasma enhanced chemical vapour deposition techniques [23], graphite oxide reduction [24],,, etc.

Graphite oxide was first prepared by B. C. Brodie, who treated it with a mixture of KClO₃ and nitric acid [25]. Later, Hummers and Offeman used a mixture of sulfuric acid, sodium nitrate, and potassium permanganate to oxidize graphite [26]. Recently, many papers reporting the modification of the Hummers methods have been published [27]. For instance, Staudenmaier method of oxidation of graphite by HNO₃/H₂SO₄ in 1:2 volume ratios, in the presence of KClO₃, was carried out within 5 days. Daniela C. Marcano and coworkers found that while using NaNO₃, one can improve the efficiency of the oxidation process by increasing the amount of KMnO₄, and perform the reaction in a 9:1 mixture of H₂SO₄/H₃PO₄ [28, 29].

Recently, several approaches to fabricating sensors based on graphene materials have been reported; among them, the use of multilayer graphene to act as a detector of NO₂ gas (Hong Kyw Choi and co-workers) [30], NH₃ gas sensors based on chemically reduced graphene oxide (Nantao Hu) [31], edge-tailored graphene oxide nanosheet-based field-effect transistors for fast and reversible electronic detection of sulfur dioxide (Fangping Shen et al) [32], two-beam-laser interference mediated reduction, patterning and nanostructuring of graphene oxide for the production of a flexible humidity sensing device (Li Guo and co-workers) [33], hydrogen sensing using Pd-functionalized multilayer graphene nanoribbon networks (Jason L. Johnson) [34], graphene sheet for Carbon dioxide gas sensor (Hyeun Joong Yoona) [35], ultrahigh humidity sensitivity of graphene oxide (Hengchang Bi) [36], Ultraviolet, visible, and near infrared photoresponse properties of solution

processed graphene oxide (Xiang Qi, et al.) [37],,,, etc.

In this paper, we will report a study the graphene oxide sensing response to (CO, H₂) gases and 375 nm UV light. The graphene oxide was prepared using the Improved Hummers method and characterized by Transmission Electron Microscopy (TEM) and Scanning Electron Microscope (SEM).

The device was operated at room temperature for detecting different gas concentrations (60, 120, 240, 480 and 960 ppm) of the (CO, H₂) gases and 375 nm UV light in a natural environment. This device showed high responsiveness and sensitivity.

2. Experimental section

Synthesis of Graphene Oxide

Graphene oxide was synthesized using an improved Hummer's method. This method produces graphene oxide from graphite powder. Graphene oxide nanosheets were prepared from graphite flakes using an improved Hummer's method reported by Marcano, et al. Briefly [29], 1 g of graphite flakes and 6 g of KMnO₄ were added into the 100ml mixture of concentrated H₂SO₄/H₃PO₄ (9:1). The resulting mixture was stirred at 50°C for 12 h. Afterwards, the reaction was then cooled overnight and poured onto ice (around 200mL) with 30% H₂O₂ (1mL). The resulting mixture was washed with HCl and H₂O respectively, followed by filtration and drying, graphene oxide sheets were thus obtained [29]. Adding deionized water and subjecting it to ultrasonic gives a stable aqueous dispersion of graphene oxide. The resulting graphene oxide solution had a concentration of 2 mg/ml.

Materials characterization

Transmission electron microscopy (TEM) was used to establish the morphology and to evaluate graphene oxide sheet size using (JEM 1011, operating at 100 kV and 3000x magnification). High-resolution scanning electron microscopy (SEM) also provided us with evidence of graphene oxide thin sheets.

Device fabrication:

One of the advantages of the graphene oxide is its easy dispersability in water and other organic solvents due to the presence of the oxygen functionalities [37]. These advantages allow to easily fabricating the device by dispersing graphene oxide uniformly on interdigitated electrodes. We fabricated our device by depositing the aqueous dispersion of graphene oxide by drop-casting on to the interdigitated Au electrodes with Alumina substrate (20µm gap between Au electrodes) as seen in Fig.1, then drop-casting the

solution of graphene oxide and drying it at 80°C for 5 hours in the air.

3. Result and discussion

The electronics microscope image in Fig. 1 shows the basics of the sensor device fabrication provided with Au interdigitated electrodes placed upon an alumina substrate and the the morphology of graphene oxide (already been broken down into small pieces) on the Au interdigitated electrode. The two-dimensional structure of graphene oxide was confirmed by the obtained TEM image see Fig. 2, and the morphologies of the graphene oxide sheets were observed under scanning electron microscope (SEM) in Fig.3. This synthesis of GO may be significant for appropriate purification and large-scale production of GO as well as the construction of the sensor device, in addition the aqueous dispersion of graphene oxide exhibited brown which was more significant in relatively low concentrations. Graphene oxide materials are deposited on the patterned substrate by 80 µL drops-casting to make electrical contacts between adjacent electrodes.

The thickness of the prepared aqueous dispersion of GO sheets was measured from the height profile of the Atomic force microscopy (AFM) image, Fig. 4, is about 2 nm, which is consistent with the data reported in the literature, indicating that the morphology of the show the real aqueous dispersion of graphene.

The gas sensor experimental setup is shown in Fig. 5. The gas sensor device was placed in the middle of the crystal tube of a tubular furnace. The furnace heating system fixed to the desired room temperature, the mixing chamber kept at ambient temperature and pressure. Their gas flow rates were controlled by Mass Flow Controller (MFC) interfaced to the personal computer equipped with LabVIEW software controls all the operations related to the gas protocol and to data acquisition. The measurement was displayed in a LabVIEW graphical user interface (GUI) and recorded as an MS Excel format.

The UV photodetector experimental setup, first connect the sensor device with DC voltage bias from the power supply, fixed UV LED above of the device sensor inside the darkness chamber kept at ambient temperature and pressure to verify the true test conditions of the photodetection. The input of the UV LED it is a square wave from signal generator and the output of the sensor device connected with the Agilent B1500A Semiconductor Device Analyzer to record the output data in both MS Excel format and JPEG figures.

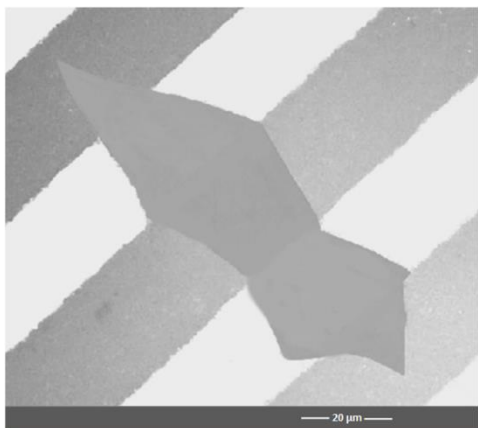


Fig. 1. The real image of the fabrication sensor device

The electrical measurement was performed by an Agilent B1500A Semiconductor Device Analyzer at room temperature and air atmosphere. The current-voltage (I-V) characteristic was studied by measuring the voltage with varying current at room temperature ($T \sim 30^\circ\text{C}$) in order to see the electrical characteristics of the sensor device. The current-voltage (I-V) between the graphene oxide and Au electrode contacts is shown in Fig.6. It demonstrates that the graphene oxide devices exhibited a linear I-V curve, which implies an ohmic contact between graphene oxide sheets and Au electrodes. As well the Fig. 7 shows the dark current and photocurrent under the illumination 375 nm light at room temperature. The dark current of the graphene oxide ultraviolet detector is $50 \mu\text{A}$ under -5 V to 5 V bias and the light current is about 9 mA . From the curves, we can clearly see that, upon the 375 nm UV illumination, the photodetector exhibited a remarkable increase in the current which is indicated that the obtained graphene oxide nanowires UV photodetector has the characteristic good sensitivity [38]. Both result of the I-V curves in the dark and under UV illumination are linear I-V curves. The linear relationship of the characteristics reveals that the contact has good Ohmic character.

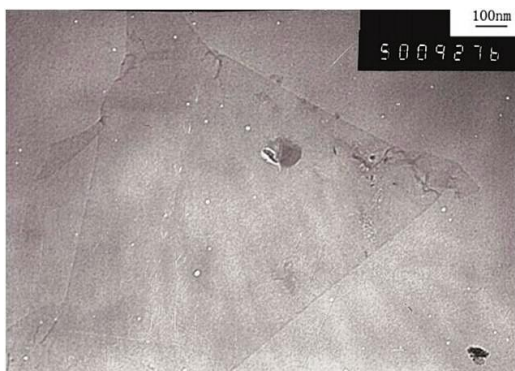


Fig. 2. TEM of the graphene oxide

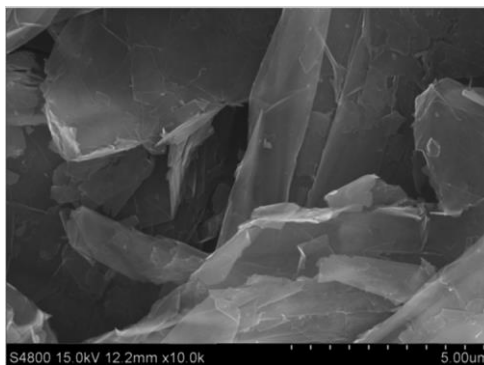


Fig. 3. SEM of the graphene oxide

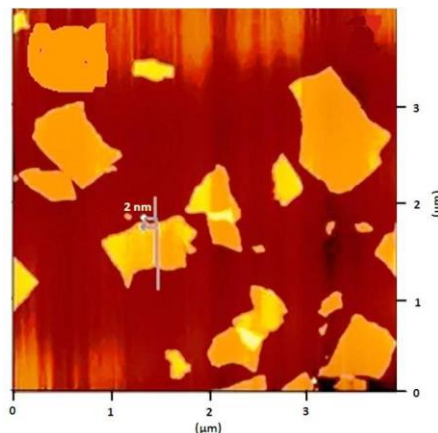


Fig. 4. The AFM image of the graphene oxide

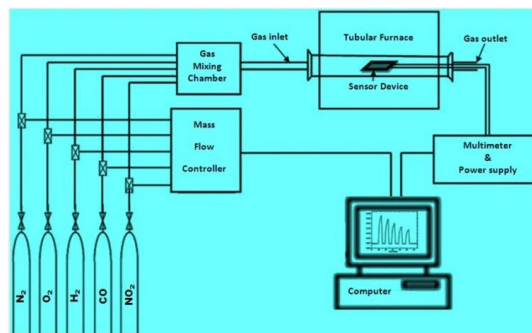


Fig. 5. Simple schematic diagram of a set up for the gas sensing characteristic measurement

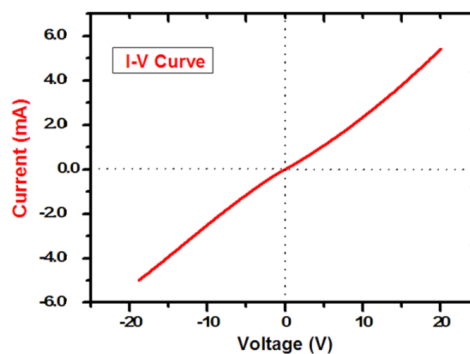


Fig. 6. I-V curve of the sensor device based on the graphene oxide

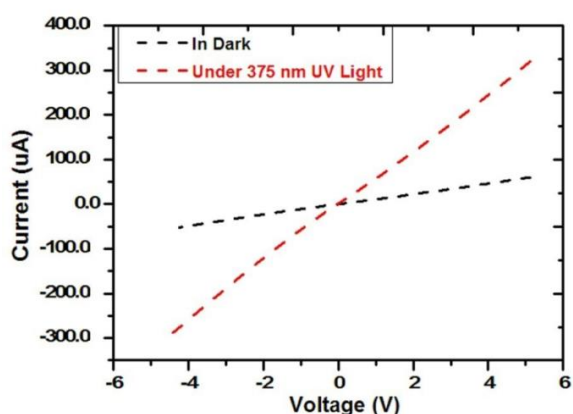


Fig. 7. I-V curve of the sensor device based on the graphene oxide in dark and under UV light

4. The gas sensing

The mechanism of graphene oxide production was mainly the generation of oxygen containing groups on graphene sheets, when electron-donating CO and H₂ gas molecules are in the atmosphere around the sensor the CO and H₂ molecules are adsorbed on the surface of the graphene oxide sheet channel and donate electrons to it. This process causes a quite significant change in the electrical properties of the graphene oxide. These strong adsorption effects stem from the inherent properties of gas molecules and the bonding characteristics between these molecules and the graphene oxide leading to changes in the conductance of graphene oxide.

The graphene oxide devices became highly responsive to CO and H₂, which was most likely due to the recovery of many graphitic carbon atoms as active sites for target gas adsorption. Possibly vacancies or small holes on the graphene oxide sheets these may also serve as adsorption sites for gaseous molecules.

The typical dynamic responses (resistance versus time) of the graphene oxide gas sensors to CO and H₂ in the dry air at various CO and H₂ gas concentrations (960, 480, 240, 120 and 60 ppm), measured at room temperature are shown in Fig. 7 and Fig. 8 respectively. The sensor was periodically exposed to clean dry air flow to record a base value of the sensor conductance, different concentration (960, 480, 240, 120 and 60 ppm) from different gases were mixed with air to register a sensing signal, and clean air flow again to recover the device.

The sensitivity can be defined by

$$S(\%) = \frac{R_{Air} - R_{Gas}}{R_{Air}} \times 100\%$$

Where R_{Air} and R_{Gas} are the resistances of graphene oxide in air and ambient gas, respectively. In this

experiment, the S under exposure of 960 ppm CO and H₂ are 22.83% and 17.12%, respectively.

The sensor resistance increases in exposure to CO and H₂, revealing P-type semiconducting behaviour of the graphene oxide gas sensors. The degree of the resistance increase depends on the gas concentration. The peak time for the higher resistance value became shorter as the gas concentration decreased. The variation in resistance was measured upon the exposure to the CO and H₂ concentrations ranging from 60 to 960 ppm. The graphene oxide gas sensor responded to 60 ppm of CO and H₂ at room temperature with a high sensitivity and the sensitivity start increase when we are increasing the gas concentrations to 960 ppm.

It is well known that in the gas detectors based on metal oxide semiconductors the operation of releasing and trapping electrons from sensing layer is responsible for the gas sensing behaviour.³⁶ In the cases of CO and H₂ gases, the CO and H₂ gases react with the oxygen species adsorbed on the active layer surface of the sensors and releases electrons back from the trapped states to the conduction band of graphene oxide, leading to an increase in electron density in the graphene oxide based active layer and a decrease in sensor resistance. It is clear from the figures (8 and 9) that the graphene oxide behaves as a p-type semiconductor [39].

Upon the introduction of target gas (CO and H₂), the sensor resistance went up, i.e., the conductance of the sensor decreased; when the CO and H₂ flow was turned off and the air flow restored, the device re-established its conductance in about 2 min. Five cycles were repeated in figures (8 and 9) and the signal was fairly reproducible. The sensing signal strength (proportional to the spike height with the target gas (CO and H₂)) was dependent on the target gas concentration as it decreased with increasing target gas concentrations from 960, 480, 240, 120 and 60 ppm, assuming a linear relationship between conductance change and target gas concentrations.

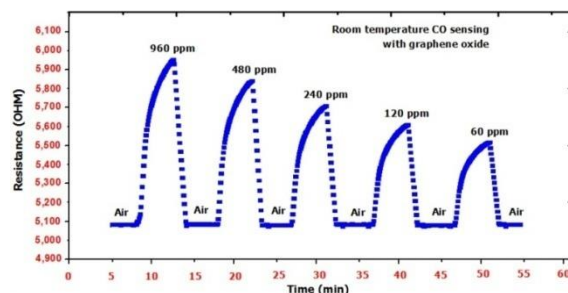


Fig. 8. The Resistance response curve of the graphene oxide gas sensor to various CO gas concentrations in dry air at the room temperature

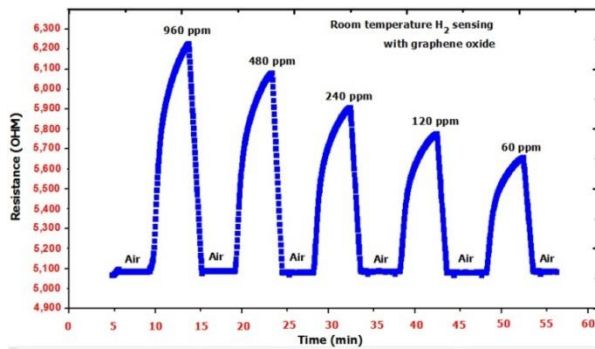


Fig. 9. The Resistance response curve of the graphene oxide gas sensor to various H_2 gas concentrations in dry air at the room temperature

The response time, as conventionally defined [40]. The Response time is defined as a time taken to reach 90% of the saturation value of sensor response when the sensor is exposed to the CO and H_2 was found to be fast about 3 and 2 minutes respectively, alongside a good sensing performance, with high sensitivity depending on the gas concentration in the dry air measured at room temperature [41]. A linear increase in the sensor response with increasing gas concentration is clearly seen for CO and H_2 . The transient response was equilibrated also the base resistance of the sensor is fully recoverable [42]. The sensing performance of the devices reported here is very encouraging for practical applications when considering the simplicity and low cost to fabricate these devices and the potential opportunities for optimization. The sensing performance of the reported device is attributed to the effective absorption of the target gas (CO and H_2) on the surface of p-type graphene oxide. CO and H_2 are strong oxidizing and reducing agent; therefore, electron transfer from graphene oxide to adsorbed gas target leads to an enriched hole concentration and enhanced electrical conduction in the graphene oxide sheet. Further investigation is needed to understand the mechanisms associated with the recovery of graphene oxide from (CO and H_2) exposure and to find effective measures to response and recovery time of graphene oxide can be used practically for detecting repeatable target gas. The initial resistance of the GO gas sensor in dry air was about 5080 OHM at the room temperature, whereas its resistance increased abruptly when it was exposed to CO/ H_2 gas. The resistance of the GO gas sensor increased after each CO/ H_2 gas injection cycle and its response and recovery process can be established. Recovery time is defined as a time taken to drop back to 10% of the sanitation value of sensor response when the sensor is placed in clean air (to initial value) was found to be fast about 2 minutes for both CO and H_2 .

All of these sensing phenomena show five sensing cycles, these sensing performance are superior to that shown in Fig. 8 and Fig. 9, however, an unusual resistance increase was observed at the beginning of

the (CO and H_2) exposure in each cycle showing more stable device with fast response and recovery time for both CO and H_2 sensing performance.

The Fig 10 shows the relationship between CO/ H_2 concentrations and sensitivity observed for the gas sensors at room temperatures. The sensitivity of the sensors increased as CO/ H_2 concentrations. These concentrations were chosen to observe clearly the different sensor response curves towards these two types of gases. It is well known that the sensitivity of the sensor based on sensing was mainly determined by the interactions between the target gas and the sensing surface. Furthermore, it can ensure that the surface area of the sensing materials is greater, and the stronger interaction and the higher response can be expected. Thus, our GO based sensor demonstrated good response to CO and H_2 at the room temperature.

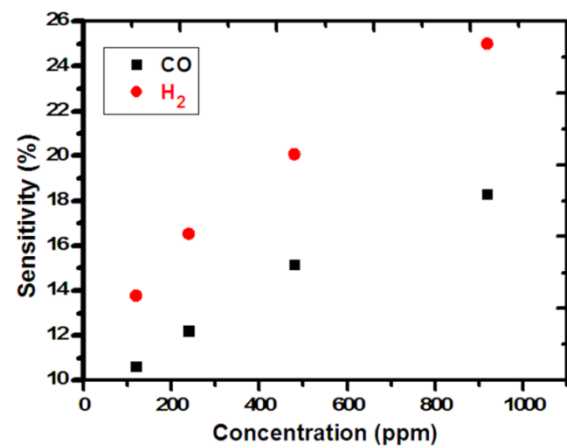


Fig. 10. Sensitivity of the sensor at room temperature for various CO and H_2 gas concentrations

The graphene oxide sensor has higher responsibility and sensitivity with faster response time and recovery time to both CO and H_2 gas sensing [35].

5. The UV photodetection

The photocurrent was measured under a small bias voltage $V_{\text{bias}} = 2\text{V}$ and 4V . The UV source was turned on and off in 5 seconds. The plot is in the Fig. 11 shows a cycle of the UV being turned on and off to demonstrate the reproducibility of the data with time, sensitivity and the stability of the fabricated device. Finally, the photonic characteristics of the graphene oxide photodetectors were measured by detecting the current change under illumination from 375 nm UV light. Fig. 11 shows the conductance modulation of air-exposed graphene oxide under UV illumination. When the UV lamp was turned on, the current steeply increased quickly due to the generation of a photocurrent, but gradually decreased to the dark current level with a few of seconds time constant [43,44]. The current increase at the beginning of the

illumination cycle is due to the electron hole pair generated in the graphene oxide [45,46]. The gradual decrease of the current under illumination is attributed to the gradual shift of the charge neutrality level caused by photodesorption and re-adsorption of molecular species on the surface of graphene oxide.⁴³

A small response and recovery times shows good photodetector. The Response time is defined as a time taken to reach 90% of the saturation value of resistance when the photodetector is exposed to the UV. A small value of time implies a good UV photodetector. Recovery time is defined as a time taken to drop back to 10% of the saturation value of resistance when the photodetector is placed in clean air (to initial value). This value also has to be small for a good photodetector. The device responded to the illumination as soon as the source was turned "ON". After turning off the light, the photocurrent decreases with time. It can be seen that when the sensor illuminated by the light source, the current increases very fast until it reaches a steady state (4.5 mA at 2V bias and about 9 mA at 4V) indicating fast response time about 0.2 second and slowly recovers the dark current (0.2 mA at 2V bias and 0.25 mA at 4V) when the light is switched off indicating low recovery time about 0.6 second comparing with the device response time.

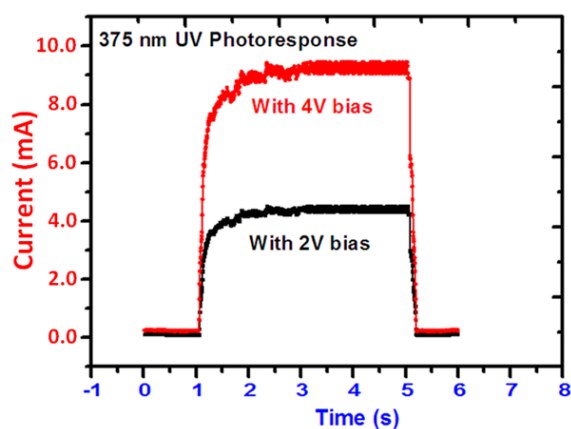


Fig. 11. Time-dependent photoresponse of the graphene oxide UV sensor at a bias voltage of (2V and 4V) under 375 nm UV illumination

The electrical conductance and sensing performance of the GO device has been studied in comparison with other's reported data in the room temperature for UV detection and CO, H₂ gas sensing [47-49]. Our device shows enhancement in electrical conductance, gas responsibility and UV detection. Thus, development of gas sensor and photodetector with high sensitivity, short response time and low cost is in great demand. One of the promising sensing materials is graphene oxide because of its unique and outstanding mechanical, thermal and electrical properties. As well the GO device shown better

performance in case sensitivity, time response and time recovery (about 70% and 0.2 second respectively) in comparison with other's reported data (about 7% to 26%, 6 to 30 minutes and 16 to 35 minutes) for sensitivity, time response and time recovery respectively [50, 51].

In the development of metal oxide gas and photo sensing for a given application, numerous factors affecting performance must be considered. Among these are sensitivity, response time, stability and environmental (e.g., temperature) effects. Some of these concerns dictate the synthesis procedure, crystal size and shape, fabrication procedure and establishing optimal operating conditions. These criteria play an important role in the design of a complete sensor system.

The most of the sensor properties depends on the equilibrium founded among the formation of oxygen vacancies and their cancellation. When the surface was activated with the gas molecules and light source with enough energy, electron-holes pairs are generated. Also UV light source generates more charge carriers and assists to enhance interacting of the surface of the sample with oxygen molecules accelerating the reactions and the subsequently formed chemical species adsorbed on the surface of metal oxide semiconductors from all these aspects it is clear that UV irradiation can affect gas detection in metal oxide semiconductors [52-54]. It can enhance the carrier generation and increasing the density of free electron-hole couple. It is also responsible for the photodissociation of the target gas and it enhances the performance of the sensor at room temperature for better future work [55].

6. Conclusion

Graphene oxide was prepared from the graphite as starting material, using the improved hummer's method. We have developed high performance and sensitive room temperature CO and H₂ gas sensors based on graphene oxide. Graphene oxide adsorbed with molecules, exhibits excellent responsive sensitivity and selectivity to CO and H₂ gases, as well as excellent sensing performance of sensors, high resistance change and fast response time. This graphene oxide sensor, with low cost, low power and easy fabrication, as well as scalable properties, shows great potential for high-sensitivity detection of CO and H₂ gas in a wide variety of concentrations of CO and H₂ gases (60, 120, 480 and 960 ppm). The fabricated photo detector showed a reproducible photoresponse to UV light. The UV response and recovery times (of 0.3 and 0.2 second respectively) of graphene oxide sheet photodetector were measured and the feasibility of the graphene oxide sheet based on photodetectors was demonstrated. A sensing mechanism is discussed based on the observed experimental results. These findings also present a

new strategy for improving the performance of graphene oxide sensors, which is a significant step toward the widespread usage of gas sensing applications of graphene oxide, based chemical sensors. Their high sensitivity, low operating temperature and low electrical power consumption may enable the construction of portable sensors. The proposed model can help to better understand gas/UV desorption and adsorption processes on the surface of graphene oxide sheet, which play a central role in gas sensing and photodetection.

Acknowledgments

The authors gratefully acknowledge financial support of National Natural Science Foundation of China (Nos. 60806038, 61131004, 61274076) and the National High Technology Research and Development Program of China (Nos. 2006AA040102, 2006AA040106).NSF China 61131004.

References

- [1] Satish Bykkam, Venkateswara Rao K, Shilpa C. H. Chakra, Tejaswi Thunugunta, *International Journal of Advanced Biotechnology and Research*, **4**, 142 (2013).
- [2] Jian Li, Xiaoqian Cheng, Alexey Shashurin, Michael Keidar, *Scientific Research*, **1**, 1 (2012).
- [3] Cristina Vales, J. David Nunez, Ana M. Benito, Wolfgang K. Maser, *CARBON*, **50**, 835 (2012).
- [4] E. L. Wolf, *Springer Briefs in Materials*, Springer International Publishing, New York (2014).
- [5] M. F. Craciun, I. Khrapach, M. D. Barnes, S. Russo, *Journal of Physics: Condensed Matter*, **25**(42), 423201 (2013).
- [6] Shun Mao, Haihui Pu, Junhong Chen, *Royal society of chemistry advances*, **2**, 2643 (2012).
- [7] Kalim Deshmukh, S. M. Khatake, Girish M. Joshi, *Journal of Polymer Research*, **20**, 286 (2013).
- [8] Quan Zhou, Zongbin Zhao, Yongsheng Chen, Han Hua, Jieshan Qiu, *Journal of Materials Chemistry*, **48**, 24959 (2012).
- [9] Wenjing Yuan, Gaoquan Shi, *Journal of Materials Chemistry1*, **1**, 10078 (2013).
- [10] Youngbin Lee, Jong-Hyun Ahn, *World Scientific*, **8**, 1330001 (2013).
- [11] Rungang Gao, Nantao Hu, Zhi Yang, Qirong Zhu, et al., *Nanoscale Research Letters*, **8**, 32 (2013).
- [12] Yiqing Sun, Qiong Wu, Gaoquan Shi, *Energy & Environmental Science*, **4**, 1113 (2011).
- [13] Jinming Zhao, Bo Deng, Min Lv, et al., *Advanced Healthcare Materials*, **2**, 1259 (2013).
- [14] F. Bonaccorso, Z. Sun, T. Hasan, A. C. Ferrari, *Nature photonics*, **4**, 511 (2010).
- [15] Xiaoying Yang, Yinsong Wang, Xin Huang, et al., *Journal of Materials Chemistry*, **21**, 3448 (2011).
- [16] Xiuyi Lin, Jingjing Jia, Nariman Yousefi, et al., *Journal of Materials Chemistry 1*, **1**, 6869 (2013).
- [17] Xiao Huang, Zhiyuan Zeng, Zhanxi Fan, et al., *Advanced Materials*, **24**, 5979 (2012).
- [18] Yu Zhu, Dustin K. James, James M. Tour, *Graphene Oxide and Their Related Applications*, *Advanced Materials*, **24**, 4924 (2012).
- [19] Dongdong Zhang, Lei Fu, Lei Liao, et al., *Nano Research*, **5**, 875 (2012).
- [20] Yike Hu, Ming Ruan, Zelei Guo, et al., *Journal of Physics D*, **45**, 154010 (2012).
- [21] Hailong Zhou, Woo Jong Yu, Lixin Liu, et al., *Nature Communications*, **4**, 2096 (2012).
- [22] Huang, Bin Wu, Jianyi Chen, et al., *Small*, **8**, 1330 (2013).
- [23] Zheng Bo, Yong Yang, Junhong Chen, et al., *Nanoscale*, **5**, 5180 (2013).
- [24] Sasha Stankovicha, Dmitriy Dikina, Richard Pinera, et al., *CARBON*, **45**, 1558 (2007).
- [25] B. C. Brodie, *Philosophical Transactions of The Royal Society of London*, **10**, 249 (1859).
- [26] W. S Jr Hummers, R. E. Offeman, *Journal of the American Chemical Society*, **80**, 1339 (1958).
- [27] Sungjin Park and Rodney S. Ruoff, *Nature Nanotechnology*, **4**, 217 (2009).
- [28] L. Staudenmaier, *Berichte der deutschen chemischen Gesellschaft*, **31**, 1481 (1898).
- [29] Daniela C. Marcano, Dmitry V. Kosynkin, Jacob M. Berlin, et al., *American Chemical Society Nano*, **4**, 4806 (2010).
- [30] HongKyw Choi, Hu Young Jeong, Dae-Sik Lee, et al., *Carbon Letters*, **14**, 186 (2013).
- [31] Nantao Hu, Zhi Yang, Yanyan Wang, et al., *Nanotechnology*, **25**, 0957 (2014).
- [32] Fangping Shen, Dong Wang, Rui Liu, et al., *Nanoscale*, **5**, 537 (2013).
- [33] Li Guo, Hao-Bo Jiang, Rui-Qiang Shao, et al., *CARBON*, **50**, 1667 (2012).
- [34] Jason L. Johnson, Ashkan Behnam, S. J. Pearton, Ant Ural, *Advanced Materials*, **22**, 4877 (2010).
- [35] Hyeun Joong Yoon, Do Han Jun, Jin Ho Yang, et al., *Sensors and Actuators B*, **15**, 7310 (2011).
- [36] Hengchang Bi, Kuibo Yin, Xiao Xie, et al., *Scientific Reports*, **3**, 2714 (2013).
- [37] Laura J. Cote, Jaemyung Kim, Vincent C. Tung, et al., *Pure and Applied Chemistry*, **83**, 95 (2011).
- [38] Abdelrahim Ate, Zhenan Tang, *International Journal of Optoelectronic Engineering*, **4**, 6 (2014).
- [39] Shubhda Srivastava, Kiran Jain, V. N. Singh, et al., *Nanotechnology*, **23**, 205501 (2012).
- [40] George F. Fine, Leon M. Cavanagh, Ayo Afonja, Russell Binions, *Sensors*, **10**, 5469 (2010).
- [41] Renjiang L'u, Wei Zhou, Keying Shi, et al., *Nanoscale*, **5**, 8569 (2013).
- [42] K. Mukherjee, A. P. S. Gaur, S. B. Majumder, *Journal of Physics D*, **45**, 505306 (2012).
- [43] Y. Shi, W. Fang, et al., *Small*, **5**(17), 2005 (2009).
- [44] P. Sun, M. Zhu, et al., *Applied Physics Letters*, **101**(5), 053107 (2012).

- [45] J. Park, Y. H. Ahn, C. Ruiz-Vargas, *Nano Letters*, **9**(5), 1742 (2009).
- [46] G. Giovannetti, P. A. Khomyakov, et al., *Phys. Rev. Lett.*, **101**(2), 026803 (2008).
- [47] S. Basua, P. Bhattacharyya, *Sensors and Actuators B*, **173**, 1 (2012).
- [48] Ganhua Lu, Leonidas E. Ocola, Junhong Chen, *Applied Physics Letters*, **94**, 083111 (2009).
- [49] Sin Ki Lai, Libin Tang, et al., *Journal of Materials Chemistry C*, **2**, 6971 (2014).
- [50] Weiwei Li, Xiumei Geng, et al., *ACS Nano*, **5** (9), 6955 (2011).
- [51] Basant Chitara, S. B. Krupanidhi, C. N. R. Rao, *Appl. Phys. Lett.* **99**, 113114 (2011).
- [52] Chunqiao Gea, Changsheng Xie, et al., *Materials Science and Engineering: B*, **141**, 43 (2007).
- [53] Geyu Lu, Jing Xu, et al., *Sensors and Actuators B*., **162**, 82 (2012).
- [54] Irmak Karaduman, Mehmet Demir, et al., *Physica Scripta*, **90**, 055802 (2015).
- [55] J. Herrán, O. Fernández-González, et al., *Sensors and Actuators B: Chemical*, **149**, 368 (2010).

*Corresponding author: wadalroob@gmail.com